Pathology of building materials in historic buildings. Relationship between laboratory testing and infrared thermography

C. Lerma[a]✉, Á. Mas[a], E. Gil[a], J. Vercher[a], M.J. Peñalver[a]

a. Universitat Politècnica de València. (Valencia, España)
✉clerma@csa.upv.es

ABSTRACT: Study of historic buildings requires a pathology analysis of the construction materials used in order to define their conservation state. Usually we can find capillary moisture, salt crystallization or density differences by deterioration. Sometimes this issue is carried out by destructive testing which determine materials' physical and chemical characteristics. However, they are unfavorable regarding the building's integrity, and they are sometimes difficult to implement. This paper presents a technique using infrared thermography to analyze the existing pathology and has the advantage of being able to diagnose inaccessible areas in buildings. The results obtained by this technique have been compared with those obtained in the laboratory, in order to validate this study and thus to extrapolate the methodology to other buildings and materials.

KEYWORDS: Limestone; Decay; Physical properties; Thermal analysis

RESUMEN: *Patología de materiales de construcción en edificios históricos. Relación entre ensayos de laboratorio y termografía infrarroja.* El estudio de edificios históricos requiere un análisis de la patología de los materiales de construcción empleados para poder definir su estado de conservación. Habitualmente nos encontramos con humedades por capilaridad, cristalización de sales o diferencias de densidad por deterioro. En ocasiones esto se lleva a cabo mediante ensayos destructivos que nos determinan las características físicas y químicas de los materiales, pero que resultan desfavorables respecto a la integridad del edificio, y en ocasiones resulta complejo llevarlos a cabo. Este trabajo presenta una técnica para analizar la patología existente mediante el empleo de termografía infrarroja con la ventaja de poder diagnosticar zonas de difícil acceso en los edificios. Para validar este estudio se han comparado los resultados obtenidos mediante esta técnica con los alcanzados en el laboratorio. De esta forma podemos extrapolar la metodología empleada a otros edificios y materiales.

PALABRAS CLAVE: Caliza; Deterioro; Propiedades físicas; Análisis térmico

1. INTRODUCTION

Conservation measures appropriate to the building under study can only be planned and executed following an accurate diagnosis of the deterioration – including adequate and reliable information about the materials used, as well as the factors and processes involved in the deterioration (1). It is necessary to be very careful when examining historic buildings and the use of non-destructive techniques such as infrared thermographic imaging facilitates the study of materials without damaging the structure.

In the building studied, as in most historic buildings, various materials have been used. This diversity is due to architectural considerations, constructive or artistic requirements, and proximity to quarrying materials. The state of deterioration of a monument is characterised by the type, intensity, and extent of the damage.

The images in this paper show the outer walls of the Seminary-School of Corpus Christi in Valencia, Spain, comprising a stone footing course under a Valencian-style rammed earth and brick wall some 80 cm thick.

There are several methods of using infrared technology (9), although the most common are active thermographic imaging, which involves artificially heating the sample, and passive thermographic imaging, where the material or the structure is heated by sunlight. When studying large areas, such as the facades of buildings, we believe that passive thermographic imaging is the most suitable option – especially for buildings in narrow streets.

Infrared thermographic imaging was used in previous studies in relation to defects in stone materials and images were interpreted for different points of the walls (3). Areas with thermal discontinuities corresponded to defective points in the material, while points with similar temperatures represent thermal inertia, or the tendency of an element to withstand temperature changes and – depending on the characteristics of the material – dampness and damage (4). Thermographic imaging has also been used to detect dampness using multi-temporal analysis (5). Our contribution focuses on comparing laboratory and material analyses with thermographic imaging in order to corroborate the results obtained using either technique.

In this study, we used a FLIR B335 camera that produces thermographic images at a resolution of 320×240 pixels, with a temperature range of –20 to +120 °C and an accuracy of less than 50 mK NETD. The thermographic images were subsequently processed with FLIR QuickReport software, which can vary the colour palette, temperature range, distance, as well as calculate the maximum, minimum, and average temperatures in the study areas. The temperature of each pixel in the image can be exported in Excel format.

2. METHODOLOGY

The procedure involves an analysis of thermographic images of a building. We compare the results obtained from these images with laboratory tests made on the materials.

The materials analysed are traditional limestone blocks from the Valencia region, such as stone from Godella and Ribarroja (widely used for centuries in the city of Valencia) and Bateig Azul limestone (in use today).

Laboratory tests detail the characteristics of the material, such as density, porosity, chemical composition, etc., and infrared imaging reveals the thermal behaviour of these materials. The weight of the samples used in the laboratory is registered using precision scales (0.01 g).

2.1. Infrared thermography

The ability to clearly see defects in a material depends on the difference between the thermal characteristics of the material and the degree of homogeneity (6), while the thermal behaviour of a material largely depend on its characteristics (thermal diffusion, porosity, density, etc.). The emissivity value is higher than 90% for most common construction materials, and in our case we have used a default value of 0.95 so that the results of measurements can be considered reliable (7).

Passive thermography has been used in laboratory and in situ tests. According to Cañas (8), in the absence of heat from the sun, data obtained from thermographic imaging is very accurate for ceramics, stone, and adobe. However, if the sun's rays shine on a facade then the thermal response of the material is altered. The thermal images shown in this study were taken before dawn, when the material was at its coolest, and this enables us to make fewer errors when comparing data and images.

The temperature difference between materials is largely due to density and specific heat, and in particular, thermal inertia. Stone has considerable capacity to store energy and takes longer to heat or cool than materials such as brick.

We linked the thermal images with some of the properties of stone, and examined those properties that are linked to the deteriorating state of the building as they involve water circulation mechanisms in porous media.

Building materials are porous and can deteriorate through moisture penetration, compound dissolution, salt migration and crystallisation, or volumetric changes such as swelling, cracking, and flaking (2).

2.2. Test description

2.2.1. Rising dampu

The walls of the building sit on humid ground. Dampness rises through the walls due to capillary action, while drying occurs on the walls due to surface evaporation. There is normally an equilibrium between the two phenomena that generates a wet front or tide mark of capillary action.

The drying process can be divided into two stages: the first corresponds to evaporation from the surface and depends on capillary action and the nature of the solution – and is a linear function in time (13). The second stage has a much slower rate of evaporation and

corresponds to the water vapour diffusion through the porous medium towards the surface (14, 15).

The formula for capillary action is [1] (16):

$$H=2 \cdot \gamma \cdot \cos \theta / (r \cdot \rho \cdot g) \qquad [1]$$

Where, γ: surface tension, θ: contact angle, r: capillary radius, ρ: liquid density, g: gravity.

The equilibrium formula (17) between capillary action and evaporation is [2]:

$$h=S (b / (2 \cdot e \cdot \theta_w))^{1/2} \qquad [2]$$

Where, h: capillary equilibrium height; S: absorption capacity; b: wall thickness; e: evaporation rate per unit of humid surface area; θ_w: water content in the humid region (volume of water for unit volume of material).

To apply Equation [2] we use the following data (17): the absorption capacity S of the limestone is in the range (0.5–1.5) mm/min$^{1/2}$ so we chose as an average value 1.0 mm/min$^{1/2}$. The fraction of volume of porosity *f* is generally and approximately 0.25, and in the knowledge that $\theta_w=0.85f$, we assume $\theta_w=0.2$. We assume the wall to be 800 mm thick. For the evaporation rate, we assume the value of e=0.004 mm/min (a rate four times greater than the average annual potential evaporation in the UK). We ignore the action of gravity. In this way, we obtain an equilibrium height of h=0.71 m. This theoretical measure provides a reference with respect to the actual level reached at any time, as the balance varies depending on weather conditions.

The surrounding stone footing has a height between 0.5 and 1.5 m, and there are areas where the rising damp wet front reaches the rammed earth wall (Figure 1).

Tests in the laboratory were based on UNE-EN 1925:1999: 'Test methods for natural stone – determination of coefficient of water absorption by capillary action which specifies a method for determining the coefficient of water absorption by capillary action of natural stone.' In accordance with this norm, the results (see the graph in Figure 2) show the mass absorbed in grams divided by the area of the submerged base of the test area in m^2, based on the square root of the time in seconds. The graph shows two straight lines that indicate the value of C_1 on the slope of the first stage [3],

$$\text{where } C_1=(m_i – m_d) / A \cdot et_i \qquad [3]$$

With m_i: mass for moment i (g); m_d: dry mass (g); A: area of the submerged base (m^2); t_i: duration of a moment (s).

2.2.2. Salt crystallisation

Efflorescence is the crystallisation of salts on the surface of the material. A hard black scab or crust may be produced that contains various carbonaceous products of pollution (including soot and dust). Scaling, scabbing, or flaking produces laminas a few millimetres thick and parallel to the surface (10).

This is caused by salt crystals, such as potassium or sodium sulfates, commonly found in wall materials, and occurs above all in the summer. Efflorescent
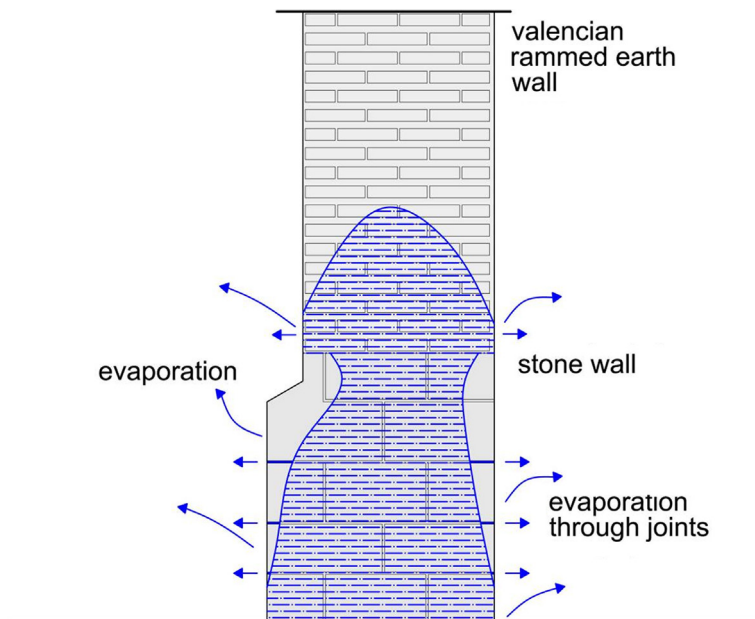

FIGURE 1.   Capillary rise in a stone and rammed earth wall.
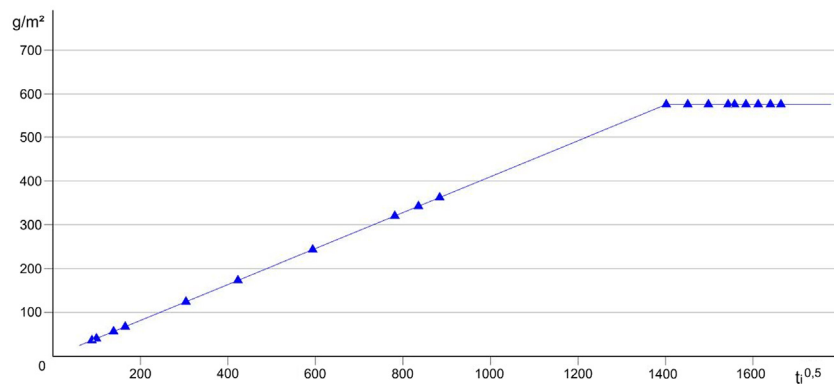
FIGURE 2.   Absorption of water by capillary action plotted against the square root of time (seconds).

salt marks indicate points of evaporation on the surface of porous materials, or with the same frequency, just below the surface and within the pores.

2.2.3. Identification of the characteristics of different materials

In the laboratory, we compared two limestone samples of differing densities. One sample was from the Godella stone quarry (D_a=2.55 g/cm^3) and the other sample was from the Bateig quarry (D_a=2.21 g/cm^3). The test consisted of maintaining the samples for 72 hours at 70±5 °C, as in other procedures for natural stone, and recording with a thermographic camera the heat loss over time (in seconds). The room temperature was 24.3 °C and relative humidity was 50.3%.

2.2.4. Deterioration caused by loss of density

Density expresses the relationship between the amount of material and volume. The greater the density, the greater the conductivity exponentially (11). The apparent density is a magnitude applied to porous materials, which typically contain air gaps, so that the total density is less than the density would be if the material were compacted.

Deterioration caused by loss of density in the material has been previously studied for other materials such as wood (12).

In the laboratory, we forced the deterioration of the material by adding hydrochloric acid (25% HCl) as described by D'Orazio (22). Acid partially dissolves the limestone, and leaves insoluble residues. In this way, we decreased the apparent density of the sample.

3. RESULTS

Table 1 summarizes the results of the tests performed, both in situ and in laboratory and in some cases, theoretical.

3.1. Capillarity

3.1.1. In situ

Once a structure is damp, the factors on which drying depend are: temperature, relative humidity, microenvironment, porosity, mechanical behaviour of the material, and duration of the humid/drying cycle (23).

Figure 3 clearly shows how the curve generated by rising damp capillary action of groundwater is reflected in the infrared image.

3.1.2. In laboratory

The results of capillary water absorption test with quarry samples demonstrate that capillary action in this material is slow.

Recent experiments have shown that higher moisture content means higher material temperatures when compared with dryer parts or materials (2). The cooling effect from evaporation is evident as the temperature is lower than the surrounding temperature. Additionally, the properties of the material significantly influence the rate of evaporation and, therefore, the speed at which a material yields moisture into the atmosphere.

In laboratory tests performed following the work of Gaius (21) it can be seen that evaporation begins once a material is dampened, and the surface temperature clearly falls. As the material loses moisture, the surface temperature and the surrounding air temperature begin to equalise.

In the laboratory, we conducted an experiment that consisted of observing and recording the evolution over time of the drying process of the samples (Figure 4).

Figure 5 shows the thermographic images for three stages of the evaporation process. Of the six samples, the first two (left) correspond to curve (a); the centre two to curve (b); and the last two (right) to curve (c). In this greyscale image, black indicates

TABLE 1.   Results of tests

TEST	TYPE	MATERIAL	RESULT			
Capillarity	Theoretical	Limestone	Height 0.71 m.			
	Laboratory	Bateig	Ta=83% Evaporation Tb=88% Tc=100%			
	On site	Godella	Variable depending on weather conditions (T and RH). Height measured with thermal camera 1.30 m.			
Crystallization of salts	Theoretical	Bateig	Evaporation in colder regions, areas of salts concentration.			
	On site	Sandstone	Efflorescence T1=100% T2=94%			
		Ribarroja	Flakes T1=100% T2=56%			
Material identification	Laboratory	Godella D1=2,55	t0 100%	t1 64%	t2 57%	t3 34%
		Bateig D2=2,21	86%	50%	43%	34%
	On site	Godella D1=2,60 P: 15%	T1=80%			
		Ribarroja D2=2,64 P: 5%	T2=100%			
Density deterioration	Laboratory	Bateig D1=2,21 D2=1,91	T1=100% T2=81%			
	On site	Godella D1=2,60 D2=2,12	T1=100% T2=85%			

D: Bulk density. P: porosity. t: time. T: temperature

lower temperatures (up to 18.7 °C), and white indicates higher temperatures (room temperature is 24.3 °C). It can be seen how the two samples on the right remain at room temperature and humidity (and are consequently difficult to see). As the experiment advances, the other four samples lose moisture and so their temperatures approach room temperature.

Figure 6 (left) shows the moisture content as a percentage of the dry weight of the six samples, and illustrates how weight loss evolves over time. The graph shows three curves, each curve representing the average of two samples with differing levels of moisture – and it can be seen how these samples tend to equilibrate with the moisture level in the atmosphere. Curve (a) refers to two samples that were immersed in water for 72 hours, long enough to absorb more water than the other samples; samples (b) were only immersed for 5 minutes; the (c) samples were references for room temperature (24.3 °C) and humidity (52.9%). The results are summarized in Table 1.

Figure 6 (right) also shows the change in the temperature of the samples. The curve (a) samples are wetter, take longer to evaporate the absorbed water, and therefore maintain a low temperature for longer. Curve (b) samples are drier, evaporate more easily, and the temperature begins to rise more quickly. Curve (c) samples maintain initial moisture and temperature at constant levels.
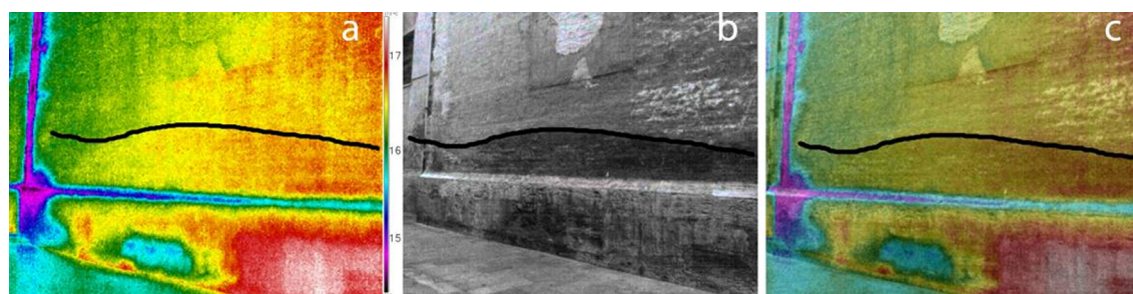

FIGURE 3.   Capillary rise of the water viewed in (a) with a thermographic camera, (b) a photograph and (c) the superimposition of (a) over (b).

FIGURE 4.   Equipment required for thermographic imaging
and sample weight.

3.2. Salt crystallisation

3.2.1. Theoretical

A distinct type of deterioration due to the crystallisation of salts in the material (20) (Figure 7) is produced in function of the speed of evaporation (V_1), and speed of water migration towards the surface (V_2).

The consequences of the accumulation of salt can block pores and capillaries through which water evaporates, pushing the wet front or tide mark upwards and so increasing moisture levels (18), reducing the capillary absorption coefficient (19). Moreover, the constant dissolution and recrystallisation of salts, as caused by changes in humidity and temperature, can damage a building material. Sodium sulphates from groundwater can be particularly destructive to buildings and monuments (24).

3.2.2. In situ

The wall in Figure 8 clearly shows rising damp on a facade that faces north and so never receives direct sunlight. Depending on the speed of evaporation (V_1), efflorescence may appear. A thermographic image shows a set of colours that represents the temperature for each point. In this figure, a temperature graph for the material is superimposed on an axis so that we can quantify temperature variations.

The facade in Figure 9 faces south and receives sunlight, therefore the speed of evaporation (V_1) is greater than in the previous case and the pathology generated is scaling – as shown in the figure.

The Ribarroja stone positioned at the doorway of the Seminary-School of Corpus Christi is suffering degradation in parallel lines that is generating a series of flakes at the surface. Not all the flakes are visible to the naked eye, but they are easily detected with thermal imaging (Figure 10). The flaking suffered by the stone involves the
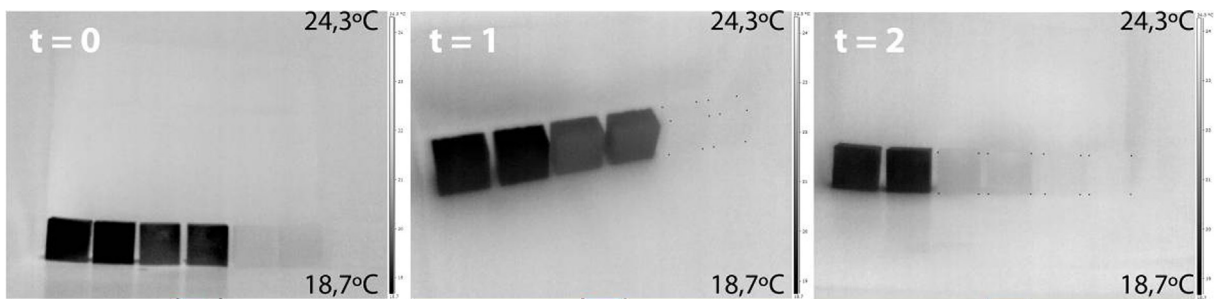

FIGURE 5.   Evaporation process of thermography.
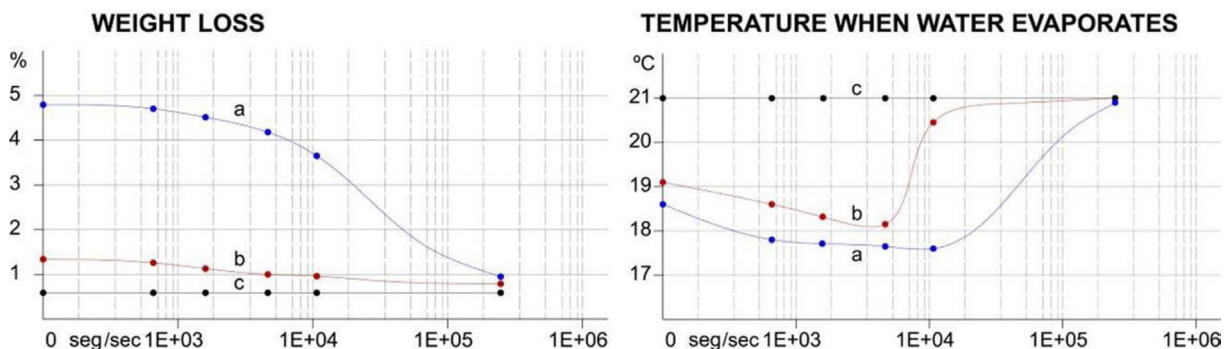

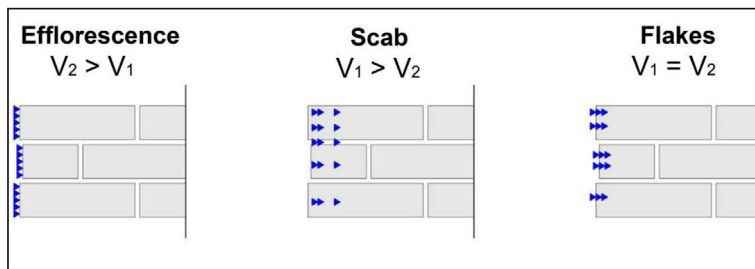FIGURE 6.   Weight loss and temperature while evaporating the water from the samples.

FIGURE 7. Material deterioration morphology cause by salt crystallization.

separation of one or more layers (altered or not) of uniform thickness (several millimetres). These flakes run parallel to each other and the structural line or a fault line in the stone (10). The flakes are thin and cool rapidly.

Figure 10b shows the pathology in detail. Flakes are forming and coming loose. Where the flakes have not become detached we can see the surface of the stone, and where no flakes remain we can see the inside of the stone blocks.

3.3. Identification of the characteristics of different materials

3.3.1. In situ

Figure 11 illustrates two types of stone, the footing being made of stone from Godella (left) and stone from Ribarroja (right). The thermographic image was taken at 7:12 am, after about 12 hours without sunlight, and the air temperature was 7.3 °C. The analytical data is given in Table 2. Bearing in mind that Ribarroja stone is less porous and denser (mean values), the thermographic image shows a thermal response 20% higher than that of Godella stone (Table 1). Denser and more compact stone has greater thermal inertia and better maintains a temperature.

3.3.2. In laboratory

Figures 12 and 13 show the loss of temperature (the Godella sample is on the left and the Bateig sample is on the right). It can be seen how over time this sample always registers a higher temperature, and so we can confirm that when a sample has a higher density it also maintains higher temperatures.
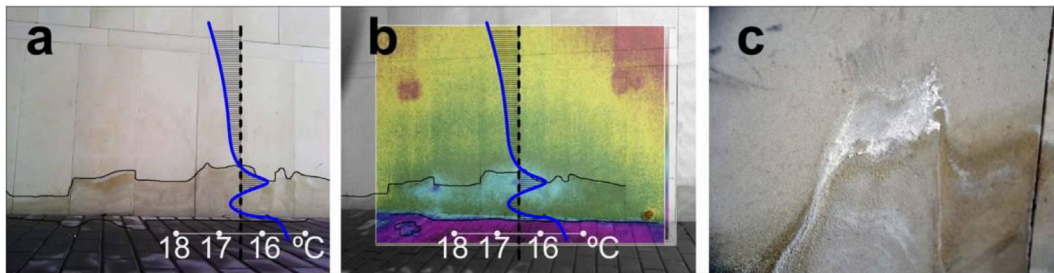

FIGURE 8. Ashlar with efflorescence, (a) thermographic image, (b) photograph and (c) superimposition of (a) over (b).
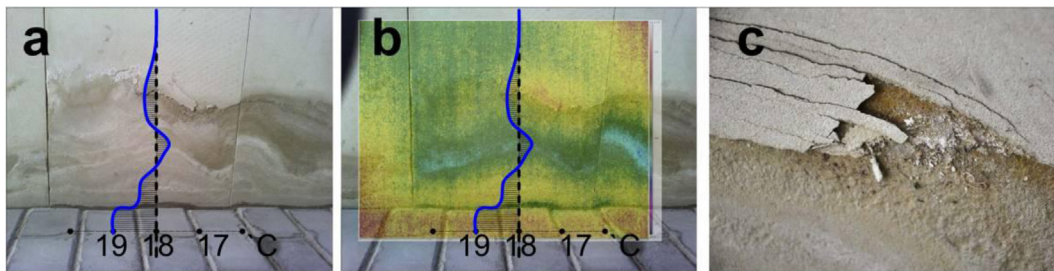

FIGURE 9. Ashlar with flakes, (a) thermographic image, (b) photograph and (c) superimposition of (a) over (b).
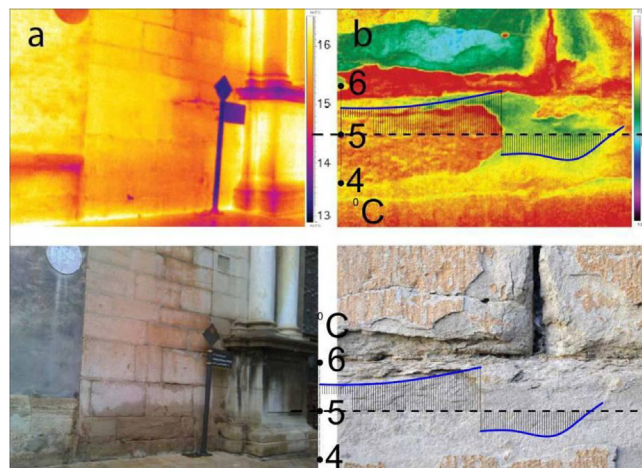
FIGURE 10. General view (a) and detail (b) of an instance of spalling. Thermographic images (top) and photographs (bottom).
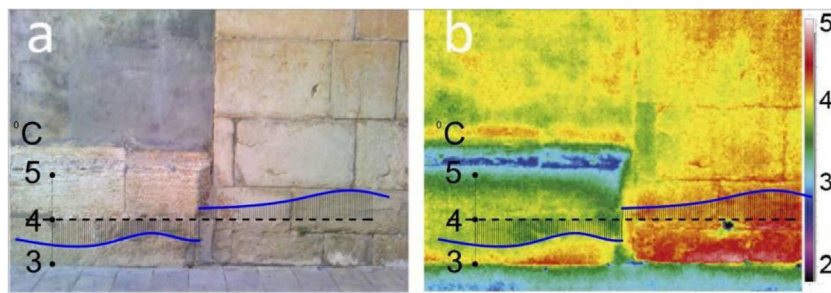

FIGURE 11. Comparison between Godella and Ribarroja stone. Photograph (a) and thermographic image (b).

3.4. Deterioration caused by loss of density

3.4.1. In situ

In Figure 14 we can see an area of the stone footing made from Godella stone. All the blocks are of the same type of stone and positioned facing west, but in the left part of the images it can be seen that alveolisation has occurred. Temperature and humidity conditions were identical as the thermographic images were taken at the same time. The thermographic images show how the temperature in the damaged area is reduced by 15%, since the left area has an average temperature of 4.1 °C and the right area a temperature of 4.8 °C (Table 1).

3.4.2. In laboratory

We moistened the samples and then left them to evaporate. We found that the degraded sample had a lower temperature. Even newly moistened degraded samples showed lower temperatures (Figure 15 and Table 1). Sample 22 was not moistened, unlike samples 23 and 24.

4. DISCUSSION

Passive infrared imaging, which takes into account the cyclical heating affect of the sun, can provide considerable information on building materials and their conservation status.

TABLE 2. Identification of different materials for their characteristics

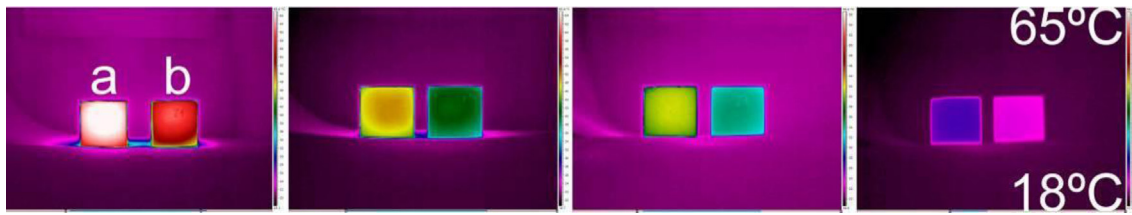| SAMPLE	GODELLA (LEFT)	RIBARROJA (RIGHT)
Average relative density	2.60 (g/cm³)	2.64 (g/cm³)
Average porosity	15%	5%
Temperature	80% (3.27 °C)	100% (4.07 °C)

FIGURE 12.   Thermography of temperature loss of two samples with different density.
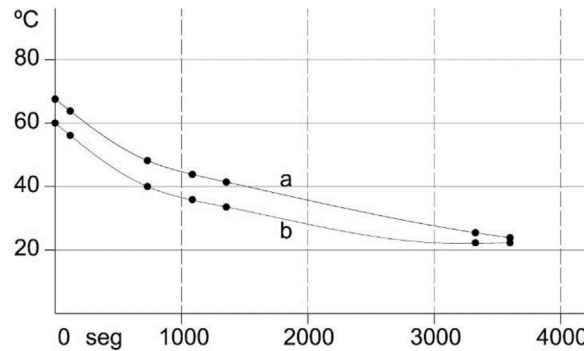

FIGURE 13.   Temperature loss of two samples with different density.

We have confirmed in the laboratory that rising damp, or capillary water action through walls, is generally a long process and tends to stabilise according to the environmental conditions for evaporation and the diffusion properties of the material. In the studied case, the average theoretical equilibrium height is 0.7 m (Table 1). The height reached by the wet front can be seen in the thermographic image – as well as the position reached in each moment (Figure 8).

In the laboratory, the cooling effect of evaporation and its relation with the temperature of the material was confirmed. It was shown that at the beginning of the process the temperature falls significantly because of the transformation from liquid to gas. Over time, the material loses humidity and its temperature tends to equalise with the air temperature.

The capillary action of rising damp is linked to salt precipitation. In cases where salts reach the surface
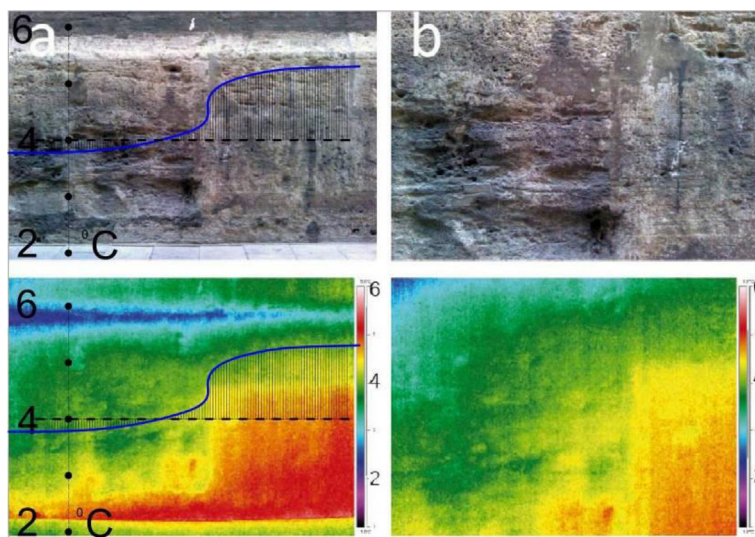

FIGURE 14.   General view (a) and detail (b) of the socle with clear superficial erosion. Photographs (top) and thermographic images (bottom).
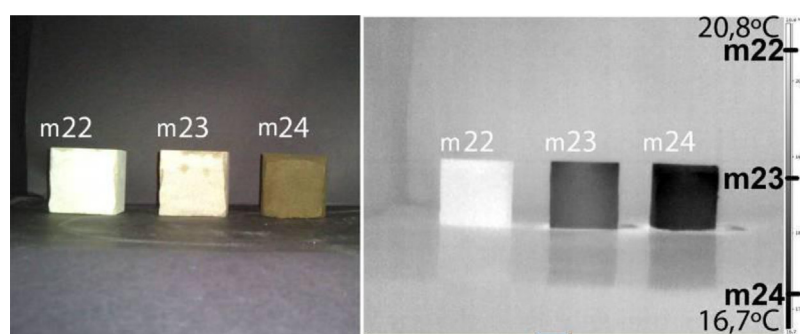
FIGURE 15.   Photography and thermography of 3 samples, 23 and 24 just moistened.

(efflorescence) or just below the surface (scaling) differences in temperature are recorded because the stone no longer has same density as the rest of the stone in the wall (Table 1). Infrared thermographic imaging has also been useful in the diagnosis of scaling and flaking (Figure 10). Deterioration in the form of flakes that are parallel to the surface – but slightly separated from the rest of the stone – shows a significant temperature reduction.

To identify two materials, such as two types of stone, environmental conditions must be the same (temperature and relative humidity), either at the building or in a laboratory (Figures 11 and 12), obtaining that materials with higher density and with less porosity reflect a higher temperature (Table 1).

Constant conditions must be maintained when analysing the same material, and we must consider that while the actual density is the same, apparent density differs and is closely related to porosity. In this case, thermographic images show lower temperatures for areas with lower apparent density, and therefore higher porosity (Figure 14). In the laboratory, artificial deterioration was caused by adding hydrochloric acid to a sample and it was found that the sample with the lowest density recorded the lowest temperature.

The more tests we perform, the more details we generally learn. However, destructive tests are not always appropriate because they degrade materials, and in some cases, may degrade the integrity of the building.

We can discover the thermal response of materials and their pathology using thermographic imaging technology or laboratory testing. By comparing the information obtained by both methods, we can produce a better diagnosis and observe the stages prior to deterioration and thus anticipate and initiate appropriate intervention.

5. CONCLUSIONS

Before restoring or rehabilitating a building it is necessary to study its history, the original documentation, and analyse the condition of the construction materials. In this article, we illustrate with infrared images the most important properties of deteriorated stone materials.

Deterioration in important historical buildings (such as the formation of efflorescence, flaking, powdering, and alveolarisation) requires an analysis that should begin with a diagnosis and survey of the building.

Thermographic imaging can help detect these deteriorations and create a sustainable approach that avoids the use of destructive methods.

A large part of the damage caused to building materials is due to the effect of rainwater. We can observe the cooling effect when water evaporates from the surface of a facade, as well as identify the wet front caused by rising damp, and the height reached by dampness at any given moment.

The rise of groundwater by capillary action (rising damp) generates a wet front within the walls that can be identified by thermographic images, and the results can be compared with laboratory or theoretical results (Table 1).

When soluble salts precipitate on the surface, the local density increases and this effect can be seen in thermographic images.

The analysis shows that stone from Godella is more porous than stone from Ribarroja. The apparent density of Godella stone is less than Ribarroja stone, and this is confirmed by the thermal response. This observation enables us to state that when the apparent density is greater, the recorded temperature increases – and this is confirmed in laboratory tests. We can test different areas of the same material under the same conditions and compare the apparent density of the various areas with the thermal response in order to understand which areas have suffered the most deterioration. Areas with less apparent density (greater porosity) are shown in thermographic images to have lower temperatures (up to 15% lower).

This technique enables us to identify areas in which flakes are about to fall loose as it is easy to observe in thermographic images the effects of the reduced thickness of the flakes when compared to undamaged rock.

REFERENCES

1. Fitzner, B. en VV. AA (1996). *Técnicas de diagnóstico aplicadas a la conservación de los materiales de construcción en los edificios históricos*. Sevilla: Junta de Andalucía.
2. Válek, J.; Kruschwitz, S.; Wostmann, J.; Kind, T.; Valach, J.; Kopp, C.; Lesák, J. (2010) Nondestructive investigation of wet building material: multimethodical approach. *Journal of performance of constructed facilities*, 462–472. http://dx.doi.org/10.1061/(ASCE)CF.1943-5509.0000056.
3. Danese, M.; Demsar, U.; Masini, N.; Charlton, M. (2010) Investigating material decay of historic buildings using visual analytics with multi-temporal infrared thermographic data. *Archaeometry*, 52 [3], 482–501. http://dx.doi.org/10.1111/j.1475-4754.2009.00485.x.
4. Campbell, J.B. (1996) *Introduction to remote sensing*, 2° ed., Taylor & Francis, London.
5. Lerma, JL.; Cabrelles, M.; Portalés, C. (2011) Multitemporal thermal analysis to detect moisture on a building façade. *Constr. Build. Mater.* 25, 2190–2197. http://dx.doi.org/10.1016/j.conbuildmat.2010.10.007.
6. Meola, C.; Carlomagno, G.M.; Giorleo, L. (2004) The use of infrared thermography for materials characterization. *J. Mater. Process. Technol.*, 155–156, 1132–1137. http://dx.doi.org/10.1016/j.jmatprotec.2004.04.268.
7. Rodríguez Liñán, C. (2011) Inspección mediante técnicas no destructivas de un edificio histórico: oratorio San Felipe Neri (Cádiz). *Informes de la Construcción* 63, 13–22. http://dx.doi.org/10.3989/ic.10.032.
8. Cañas I. (2005) Thermal-physical aspects of materials used for the construction or rural buildings in Soria (Spain). *Constr. Build. Mater.* 19, 197–211. http://dx.doi.org/10.1016/j.conbuildmat.2004.05.016.
9. Mercuri, F.; Zammit, U.; Orazi, N.; Paoloni, S.; Marinelli, M.; Scudieri, F. (2011) Active infrared thermography applied to the investigation of art and historic artefacts. *J. Therm. Anal. Calorim.* 104, 475–485. http://dx.doi.org/10.1007/s10973-011-1450-8.
10. Ordaz, J.; Esbert, R.M. (1988) Glosario de términos relacionados con el deterioro de las piedras de construcción. *Mater. Construcc.* 38 [209], ene-feb-mar, 1988.
11. González Cruz, E.M. (2003) *Selección de materiales en la concepción arquitectónica bioclimática*. Instituto de investigaciones de la Facultad de Arquitectura y Diseño, Universidad de Zulia. Venezuela.
12. Rodríguez-Liñán, C.; Morales-Conde, M.J.; Rubio-de Hita, P.; Pérez-Galve, F. (2012) Analysis of the influence of density on infrared thermography and of the scope of this technique in the detection of internal defects in wood. *Mater. Construcc.* 62 [305], 99–113, http://dx.doi.org/10.3989/mc.2012.62410.
13. Hammecker, C. (1995) The importance of the petrophysical properties and external factors in stone decay on monuments. *Pageoph.* 145, 337–361.
14. Scherer, G.W. (1990) The theory of drying. *J Am Ceram Soc.* 73, 3–14.
15. Freitas, D.S. (2000) Pore network simulation of evaporation of a binary liquid from a capillary porous médium. *Transp. Porous Media.* 40, 1–25. http://dx.doi.org/10.1023/A:1006651524722.
16. Rirsch, E.; Zhang, Z. (2010) Rising damp in masonry walls and the importance of mortar properties. *Constr. Build. Mater.* 24, 1815–1820. http://dx.doi.org/10.1016/j.conbuildmat.2010.04.024.
17. Hall, C.; Hoff, W.D. (2002) *Water transport in brick, stone and concrete*. London: Spon Press.
18. Oliver, A. (1988) *Dampness in buildings*. Oxford: BSP Professional Books.
19. Buj, O.; López, P.L.; Gisbert, J. (2010) Characterization of pore system and their influence on decay rates caused by salt weathering on limestones and dolostones quarried in Abanto (Zaragoza, Spain). *Mater. Construcc*, 60 [299], 99–114, http://dx.doi.org/10.3989/mc.2010.50108.
20. Rossi-Manaresi, R. (1988) *Degradación del Patrimonio*. Conferencia celebrada en la Facultad de Geografía e Historia. Valencia.
21. Gayo, E.; De Frutos, J.; Palomo, A.; Massa, S.A. (1996) Mathematical Model Simulating the Evaporation Processes in Building Materials: Experimental Checking through Infrared Thermography. *Building and Environment*, 31 [5], 469–475. http://dx.doi.org/10.1016/0360-1323(96)00007-8.
22. D'Oracio, M.; Munafò, P. (2013) A methodology for the evaluation of the hygrometric and mechanical properties of consolidated stones. *International Journal of Architectural Heritage*. http://dx.doi.org/10.1080/15583058.2012.756078.
23. Binda, L.; Gardani, G.; Zanzi, L. (2010) Nondestructive testing evaluation of drying process in flooded full-scale masonry walls. *J. Perform. Constr. Facil.* 24, Sp. Issue: Flood Impact to Heritage Structures, 473–483. http://dx.doi.org/10.1061/(ASCE)CF.1943-5509.0000097.
24. De Clercq, H. (2008) *Proc. Conference on salt weathering on buildings and stone sculptures*. Copenhagen: Tech University of Denmark.